

MODELING COFILIN MEDIATED REGULATION OF CELL MIGRATION AS A BIOCHEMICAL TWO-INPUT SWITCH

Christian Breindl^{*,1,2}, Steffen Waldherr^{*,2}, Angelika Hausser^{**}, and Frank Allgöwer^{*}

^{*} Institute for Systems Theory and Automatic Control,
Universität Stuttgart, Pfaffenwaldring 9, Stuttgart, Germany

^{**} Institute of Cell Biology and Immunology,
Universität Stuttgart, Allmandring 31, Stuttgart, Germany

Abstract

Cell migration plays an essential role in many physiological processes such as embryogenesis, immune response, and wound healing. However, increased cell motility also contributes to invasion and metastases of tumor cells. Therefore, understanding the intracellular mechanisms which regulate cell migration is an important issue. In this paper a mathematical model describing the regulation of cofilin, which is a direct regulator of cell motility, is developed. The mathematical model is used to study the effects of different signaling stimuli on cofilin activity. In particular, the model analysis predicts that cell migration can be stopped reliably by a specific combined stimulation of the cofilin regulatory network. This hypothesis thus proposes a mechanism how cells may sustainably be kept at a fixed place without much signaling effort.

Keywords

cell migration, mathematical modeling, cofilin regulation, bifurcation analysis, bistability

Introduction

Cell migration plays an important role in multicellular organisms. It is essential for tissue formation during embryonic development, wound healing and immune response. However, increased cell motility also contributes to invasion and metastases of tumor cells. Therefore, understanding the intracellular mechanisms by which cell migration is controlled can contribute to various fields such as the development of new therapeutic strategies.

The coordinated polymerization of actin filaments is the basis for cell motility. This process is responsible for the formation of the *lamellipodium* and *filopodium*, which are the protrusive structures at the leading edge of a migrating cell and function as anchors or antennae for cell movement (Mattila and Lappalainen, 2008). In particular, turnover of filaments by dissociation and association of actin molecules at the pointed and barbed ends, respectively, underlies the propulsive forces required for cell migration (Mogilner and Edelstein-Keshet, 2002). Actin filament turnover is controlled by several signaling proteins.

An important regulatory protein is cofilin, a member of the ADF/cofilin family, which can bind to actin filaments, thereby destabilizing them and thus increasing actin turnover. Cofilin activity is regulated by phosphorylation: the phosphorylated form is inactive, and it was observed that cells with an increased level of phosphorylated cofilin were unable to generate actin-based lamellipodia

(Jovceva et al., 2007) and therefore showed reduced motility. The phosphorylation level of cofilin is controlled by two regulatory proteins: the LIM kinases (LIMK), which phosphorylate and thereby deactivate cofilin, and the slingshot (SSH) family of phosphatases, which activate cofilin by direct dephosphorylation (Huang et al., 2006).

While actin polymerization is a well-studied and frequently modeled process (see e.g. Mogilner (2006) for a review), the regulation of cofilin has to our knowledge not been addressed with respect to mathematical modeling. The aim of this paper is to construct and analyze a mathematical model for the cofilin signaling network in order to further understand the role of cofilin regulation in cell migration. We consider the activity of two signaling proteins related to cell migration, namely Pak4 and protein kinase D (PKD) as inputs to the network. By bifurcation analysis we show that these two inputs may interact in a biologically interesting way. Our model predicts that for appropriate parameter values, cell migration can be decreased and kept at a low rate by an adequate combination of the two inputs, namely a short but high stimulation with Pak4 together with a low but enduring stimulation with PKD. A similar effect for another signaling network related to cell migration has been observed previously (Busch et al., 2008), suggesting that such a combination of inputs plays a generally important role in the regulation of cell motility.

Mathematical model of cofilin regulation

As a basis for the model development, let us first discuss the biochemistry of cofilin regulation in more detail.

¹ Corresponding author (breindl@ist.uni-stuttgart.de)

² Both authors contributed equally to this work.

Cofilin 1/2 can be phosphorylated at Ser2/Ser3, respectively, thereby loosing its ability to bind and depolymerize actin in its phosphorylated form (Bamburg, 1999; Agnew et al., 1995). Therefore, we refer to unphosphorylated cofilin as active cofilin. LIM kinases (LIMK1, LIMK2) act as direct kinases for cofilin. It was found that LIMK1 and LIMK2 are activated by phosphorylation at Thr508 and 505, respectively, through the p21-activated kinase Pak4 (Arber et al., 1998; Edwards et al., 1999). Furthermore, Soosairajah et al. (2005) observed that LIMK1 undergoes autophosphorylation at several serine residues after initial activation by Thr508 phosphorylation. For the model developed in this paper, we assume that the active form of LIMK is phosphorylated at the activating threonine and additional serine residues.

On the other hand, members of the SSH family were identified as cofilin phosphatases. SSH phosphatases dephosphorylate cofilin at Ser3 and thus restore its ability to sever actin filaments (Niwa et al., 2002; Nagata-Ohashi et al., 2004). Soosairajah et al. (2005) also reported that SSH is a phosphatase for LIMK dephosphorylating it at Thr508 and thereby decreasing its kinase activity towards cofilin. Furthermore, Soosairajah et al. (2005) and Nagata-Ohashi et al. (2004) found that the phosphorylation of SSH1 inhibits its phosphatase activity towards cofilin and LIMK. It was demonstrated that the adapter protein 14-3-3 binds to phosphorylated SSH1 and thus inhibiting the interaction of SSH1 with filamentous actin, which results in a reduction of the SSH1 phosphatase activity. Protein kinase D (PKD) negatively regulates cell migration (Eiseler et al., 2007), most likely by direct phosphorylation of SSH1 (Peterburs et al., under review). Additionally, we assume that SSH and LIMK are dephosphorylated by phosphatases not included in the model. The biochemical network resulting from these interactions is depicted in Figure 1.

Based on the constructed biochemical reaction network, we now develop a mathematical model based on ordinary differential equations. To this end, all reaction rates are modeled by Michaelis-Menten rate laws. We introduce the state variables Cof and CofP for the amount of unphosphorylated and phosphorylated cofilin, respectively, SSH and SSHP for unphosphorylated and phosphorylated SSH, and LIMK, LIMKP and LIMKPP for non-phosphorylated, singly phosphorylated (Thr505/508), and multiphosphorylated (additional serines) LIMK, respectively. Since protein turnover is neglected in the model, we have three conservation relations

$$\begin{aligned} \text{CofP} &= C - \text{Cof} \\ \text{SSHP} &= S - \text{SSH} \\ \text{LIMKPP} &= L - \text{LIMK} - \text{LIMKP}, \end{aligned} \quad (1)$$

where C , S , and L are the total amounts of cofilin, SSH and LIMK, respectively. The dynamics of the cofilin regulation network as studied in this paper are then described by the system of differential equations

$$\frac{d\text{Cof}}{dt} = v_5 - v_6 \quad (2)$$

$$\frac{d\text{SSH}}{dt} = -v_7 + v_8 \quad (3)$$

$$\frac{d\text{LIMK}}{dt} = -v_1 + v_2 \quad (4)$$

$$\frac{d\text{LIMKP}}{dt} = v_1 - v_2 - v_3 + v_4, \quad (5)$$

where the reaction rates v_i , $i = 1, \dots, 8$ are given in Table 1. The reaction rate numbers are according to the labeling in Figure 2.

As no parameter values are available in the literature, they had to be chosen in a biologically reasonable way. Due to lack of related experimental data, the concentration values are considered as relative values. We assume that the maximum reaction rates of phosphorylation and dephosphorylation of cofilin should be in a similar range. Equivalently, these reaction rates should also be similar for SSH and LIMK. We also assume that the amounts of SSH and LIMK are similar. The parameter values used for the analysis in the following section are summarized in Table 2.

Table 1. Reaction rates

$$\begin{aligned} v_1 &= \frac{(k_{1a} \cdot \text{Pak4} + k_{1c} \cdot (L - \text{LIMK} - \text{LIMKP})) \cdot \text{LIMK}}{k_{1b} + \text{LIMK}} \\ v_2 &= \frac{k_{2a} \cdot \text{LIMKP}}{k_{2b} + \text{LIMKP}} \\ v_3 &= \frac{(k_{3a} \cdot (L - \text{LIMK} - \text{LIMKP}) + k_{3c} \cdot \text{LIMKP}) \cdot \text{LIMKP}}{k_{3b} + \text{LIMKP}} \\ v_4 &= \frac{(k_{4a} + k_{4c} \cdot \text{SSH}) \cdot (L - \text{LIMK} - \text{LIMKP})}{k_{4b} + (L - \text{LIMK} - \text{LIMKP})} \\ v_5 &= \frac{(k_{5a} \cdot \text{Cof} \cdot (L - \text{LIMK} - \text{LIMKP}))}{k_{5b} + \text{Cof}} \\ v_6 &= \frac{(k_{6a} \cdot (C - \text{Cof}) \cdot \text{SSH})}{k_{6b} + \text{SSH}} \\ v_7 &= \frac{(k_{7a} \cdot \text{SSH} \cdot \text{PKD})}{k_{7b} + \text{SSH}} \\ v_8 &= \frac{(k_{8a} \cdot \text{SSH})}{k_{8b} + \text{SSH}} \end{aligned}$$

Table 2. Parameter values

parameter	value	parameter	value
L (total LIMK)	5	S (total SSH)	5
C (total Cof)	10		
parameter	value[1/s]	parameter	value[1/s]
k_{1a}	0.5	k_{1b}	5
k_{1c}	0.005	k_{2a}	0.5
k_{2b}	2	k_{3a}	0.6
k_{3b}	0.1	k_{3c}	2
k_{4a}	0.1	k_{4b}	0.5
k_{4c}	0.1	k_{5a}	0.3
k_{5b}	5	k_{6a}	0.1
k_{6b}	5	k_{7a}	0.8
k_{7b}	2	k_{8a}	0.1
k_{8b}	2		

Model Analysis

The dynamics of the mathematical model developed in the previous section are now analyzed. We consider Pak4 and PKD as inputs to the network. The goal of this

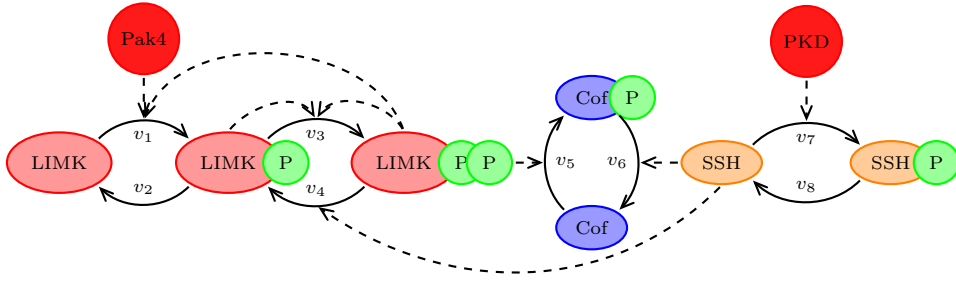


Fig. 1. Biochemical reaction network for cofilin regulation

analysis is to demonstrate that the model structure can exhibit an interesting dynamical behavior for appropriate parameter values which we refer to as a *two-input switch*. Considering the reaction network of Figure 1, one can see that the two inputs Pak4 and PKD have the same qualitative long-term effect on the amount of active cofilin. If the Pak4 stimulus is increased, the equilibrium will be shifted to higher amounts of LIMKPP which will in turn lead to a higher amount of inactive CofP. Equivalently, an increase in the PKD stimulus leads to an increased amount of inactive SSHP and the amount of inactive CofP will finally grow. As both inputs downregulate cell migration, the question is what is gained by a combined action of the two inputs. In what follows, we show that a combined stimulation can indeed lead to new dynamical behavior of the network.

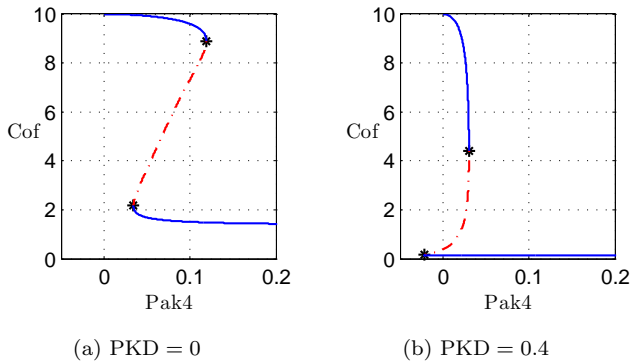


Fig. 2. Bifurcation diagrams for different PKD concentration, computed with Auto 2000 (Doedel et al., 1999)

Figure 2 shows the bifurcation diagram of the System in the Pak4-Cof plane for two different but constant values of the PKD stimulus. Figure 2(a) shows the cofilin response for $PKD = 0$. In this case, a stimulation with Pak4 may deactivate cofilin if the stimulus exceeds a certain threshold. However, after removing the Pak4 stimulus, a high level of active cofilin will inevitably recover. Some hysteresis is observed from occurrence of two saddle-node bifurcations. Increasing the input of PKD has the effect that the two bifurcation points are shifted to a lower Pak4 concentration. In particular, for a value of $PKD \approx 0.15$, the lower saddle-node crosses the vertical axis with $Pak4 = 0$, thereby inducing bistability at this value. A PKD value above the critical value, as used in Figure 2(b), will allow the system to remain in a state with low amount of Cof, if the amount of Pak4 has exceeded a value of approximately

0.03 of a sufficiently long time. Even after removing the Pak4 stimulus, high levels of Cof cannot be reached again.

In the next step, let us study the network response for different stimulation scenarios. The resulting cofilin activity courses obtained from simulation are shown in Figure 3. For the three simulations, the initial conditions were chosen as $Cof(0) = C = 10$, $SSH(0) = S = 5$, $LIMK(0) = L = 5$, with all other variables equal to zero. In Figure 3(a), the network was stimulated with a Pak4 pulse of amplitude 1 between $t = 200$ s and $t = 400$ s while the amount of PKD was set to a residual concentration of $PKD = 0.03$. The simulation shows, as expected from the bifurcation diagram, that the amount of active cofilin is downregulated. Moreover, this decrease is fast and needs less than 50 seconds. After removing the Pak4 stimulus, the concentration of active cofilin increases again, but this increase occurs at a much slower rate. This can be explained from the proximity of the trajectory to the saddle-node bifurcation at the lower Cof concentration in Figure 2(a), which is referred to as ghost effect by Strogatz (2001). Also PKD has the capacity to downregulate the amount of active cofilin. Figure 3(b) shows a simulation in which the network was stimulated with a PKD pulse of amplitude 1 between $t = 200$ s and $t = 600$ s while the amount of Pak4 was set to a residual concentration of 0.03. For the chosen set of parameters the phosphorylation of cofilin takes now place at a much slower rate and the new steady state is only reached after approximately 600 seconds. This behavior is also plausible from a biophysical view as PKD stimulation can influence the level of Cof only indirectly by inhibiting the phosphatase Slingshot.

Both cases agree qualitatively with experimental observations (Peterburs, under review), but the combined stimulation, with results shown in Figure 3(c), offers new insights. In this simulation, the amount of PKD was set to the relatively low amount of $PKD = 0.4$ which is not sufficient to drive the system into a steady state with low amount of active cofilin. If the network is additionally stimulated with the same Pak4 pulse as in Figure 3(b), cofilin is again deactivated quickly. Yet, in contrast to the scenario of Figure 3(a), after removing the Pak4 stimulus, the system does not return to its initial steady state with high amount of active cofilin. The low amount of PKD is now sufficient to keep the level of active cofilin low, which corresponds to a sustained downregulation of cell migration.

From these simulations it can be seen that the biochemical two-input switch bears an important advantage. In order to downregulate cell migration, it is not necessary that the network is enduringly stimulated with a high

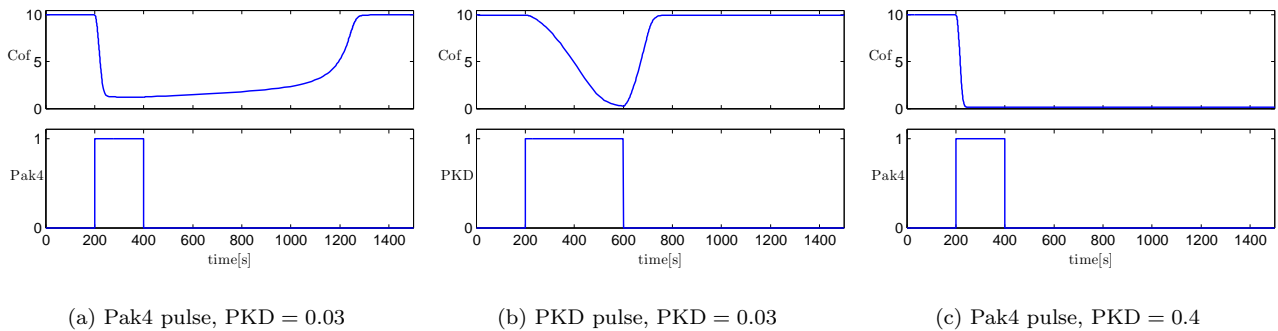


Fig. 3. System responses after stimulations

amount of either Pak4 or PKD, but a relatively short Pak4 stimulus in combination with a permanent residual activity of PKD can achieve the same result. Only by a further decrease of PKD, or by upregulation of phosphatases specific for SSH which were not considered as inputs in the model, the amount of active cofilin can increase again, resulting in a reactivation of cell motility.

Conclusions

In this paper, we developed a first mathematical model of the cofilin regulation network, which plays a major role in the process of cell migration. The model is based on many known biochemical mechanisms, but also makes use of several hypotheses about the exact interactions. Due to the lack of quantitative *in vivo* data, the parameter values are not directly related to biochemical measurements, but are chosen in a biologically reasonable way. Therefore, the model predictions should be interpreted in a qualitative way only.

Despite these restrictions, the model analysis yields interesting conclusions. Using bifurcation analysis and simulation, we have shown that the model can act as a biochemical two-input switch: the presence of a low PKD signal controls whether the inhibition of cell migration by a pulse stimulus from Pak4 is transient or sustained. This prediction constitutes a biological hypothesis that can be tested experimentally. Since loss of cellular immobility is e.g. involved in the progression of metastases, the model prediction is of medical relevance.

For future research, we envision the coupling of the proposed cofilin regulation model with mathematical models for actin polymerization and cellular propulsion. In this way, a more thorough understanding of cell migration and its regulation will be obtained.

Acknowledgments

Funding by the Center for Systems Biology Stuttgart is gratefully acknowledged. We thank Ganzhou Wang for help with the preparation of the bifurcation diagrams.

References

Agnew, B. J., Minamide, L. S., Bamberg, J. R., Jul 1995. Reactivation of phosphorylated actin depolymerizing factor and identification of the regulatory site. *Journal of Biological Chemistry* 270 (29), 17582–17587.

Arber, S., Barbayannis, F. A., Hanser, H., Schneider, C., Stanyon, C. A., Bernard, O., Caroni, P., 1998. Regulation of actin dynamics through phosphorylation of cofilin by LIM-kinase. *Nature* 393, 805–809.

Bamburg, J. R., 1999. Proteins of the ADF/cofilin family: essential regulators of actin dynamics. *Annual Review of Cell and Developmental Biology* 15, 185–230.

Busch, H., Camacho-Trullio, D., Rogon, Z., Breuhahn, K., Angel, P., Eils, R., Szabowski, A., 2008. Gene network dynamics controlling keratinocyte migration. *Mol Syst Biol* 4, 199.

Doedel, E. J., Paffenroth, R. C., Champneys, A. R., Fairgrieve, T. F., Kuznetsov, Y. A., Oldeman, B. E., Sandstede, B., Wang, X., 1999. *Auto 2000: Continuation and bifurcation software for ordinary differential equations* (with HomCont).

Edwards, D. C., Sanders, L. C., Bokoch, G. M., Gill, G. N., Sep 1999. Activation of lim-kinase by Pak1 couples Rac/Cdc42 GTPase signalling to actin cytoskeletal dynamics. *Nature Cell Biology* 1 (5), 253–259.

Eiseler, T., Schmid, M. A., Topbas, F., Pfizenmaier, K., Hausser, A., Sep 2007. PKD is recruited to sites of actin remodelling at the leading edge and negatively regulates cell migration. *FEBS Lett* 581 (22), 4279–4287.

Huang, T. Y., DerMardirossian, C., Bokoch, G. M., 2006. Cofilin phosphatases and regulation of actin dynamics. *Current Opinion in Cell Biology* 18 (1), 26–31.

Jovceva, E., Larsen, M. R., Waterfield, M. D., Baum, B., Timms, J. F., 2007. Dynamic cofilin phosphorylation in the control of lamellipodial actin homeostasis. *Journal of Cell Science* 120 (11), 1888–1897.

Mattila, P. K., Lappalainen, P., 2008. Filopodia: molecular architecture and cellular functions. *Nature Reviews of Molecular Cell Biology* 9 (6), 446–454.

Mogilner, A., Feb 2006. On the edge: modeling protrusion. *Curr Opin Cell Biol* 18 (1), 32–39.

Mogilner, A., Edelstein-Keshet, L., Sep 2002. Regulation of actin dynamics in rapidly moving cells: a quantitative analysis. *Biophys J* 83 (3), 1237–1258.

Nagata-Ohashi, K., Ohta, Y., Goto, K., Chiba, S., Mori, R., Nishita, M., Ohashi, K., Kousaka, K., Iwamatsu, A., Niwa, R., Uemura, T., Mizuno, K., May 2004. A pathway of neuregulin-induced activation of cofilin-phosphatase slingshot and cofilin in lamellipodia. *The Journal of Cell Biology* 165 (4), 465–471.

Niwa, R., Nagata-Ohashi, K., Takeichi, M., Mizuno, K., Uemura, T., Jan 2002. Control of actin reorganization by slingshot, a family of phosphatases that dephosphorylate ADF/cofilin. *Cell* 108 (2), 233–246.

Soosairajah, J., Maiti, S., Wiggan, O., Sarmiere, P., Moussi, N., Sarcevic, B., Sampath, R., Bamberg, J. R., Bernard, O., 2005. Interplay between components of a novel LIM kinase-slingshot phosphatase complex regulates cofilin. *The EMBO Journal* 24, 473–486.

Strogatz, S. H., 2001. *Nonlinear dynamics and chaos: with applications to physics, biology, chemistry, and engineering*. Studies in Nonlinearities. Westview.